agronomy

MDPI

*Article*

# Chemical Composition of *Anabasis articulata*, and Biological Activity of Greenly Synthesized Zinc Oxide Composite Nanoparticles (Zn-NPs): Antioxidant, Anticancer, and Larvicidal Activities

**Abdullah Ali Alamri [1,2], Naimah Asid H. Alanazi [3], Abadi M. Mashlawi [4], Sohair A. M. Shommo [3], Mohammed A. Akeel [5], Amani Alhejely [6], Abdel Moneim E. Sulieman [3] and Salama A. Salama [4,7,*]**

1 Physical Sciences Department, Chemistry Division, College of Science, Jazan University, P.O. Box 114, Jazan 45142, Saudi Arabia; alamri@jazanu.edu.sa
2 Nanotechnology Research Unit, College of Science, Jazan University, P.O. Box 114, Jazan 45142, Saudi Arabia
3 Department of Biology, College of Sciences, University of Ha'il, Ha'il 2240, Saudi Arabia; n.alenezy@uoh.edu.sa (N.A.H.A.); susu.shommo@gmail.com (S.A.M.S.)
4 Biology Department, College of Science, Jazan University, P.O. Box 114, Jazan 45142, Saudi Arabia; amashlawi@jazanu.edu.sa
5 Human Anatomy Department, Faculty of Medicine, Jazan University, Jazan 45142, Saudi Arabia; m.akeel@jazanu.edu.sa
6 Biology Department, Darb University College, Jazan University, Jazan 45142, Saudi Arabia; alhejely@jazanu.edu.sa
7 Zoology Department, Faculty of Science, Damanhur University, Damanhur 22511, Egypt
* Correspondence: sasalama@jazanu.edu.sa; Tel.: +966-540432176

**Abstract:** The synthesis of nanoparticles utilizing green techniques is becoming increasingly important due to its low cost, biocompatibility, high productivity, and eco-friendliness. Herein, the current work focused on the biosynthesis, characterization, and biological applications of zinc oxide nanoparticles (ZnO-NPs) from *Anabasis articulata*, including antioxidant anticancer and larvicidal properties, as well as modifications to the phytochemical ingredients. Hence, the tannin, phenolic, and flavonoid concentrations of the produced nanoparticle samples were lower than those of the original aqueous extract. When compared to the results of ascorbic acid (12.78 mg/mL), the produced extract of *A. articulata* and its zinc nanoparticles showed remarkable efficacy as antioxidant agents with $IC_{50}$ values of 27.48 and 69.53 mg/mL, respectively. A normal lung fibroblast cell line (WI-38) and three tumor cells were used to test the compounds' anticancer properties. With an $IC_{50}$ of 21.19 µg/mL, the ZnO-NPs of *A. articulata* showed the greatest cytotoxicity against HePG-2 cell lines. Additionally, *A. articulata* zinc nanoparticles showed significant cytotoxicity against MCF-7 and PC3 tumor cell lines, with $IC_{50}$ values of 30.91 and 49.32 µg/mL. The biogenic ZnO-NPs had $LC_{50}$ and $LC_{90}$ values of 13.64 and 26.23 mg/L, respectively, and are very effective against *Aedes aegypti* larval instar (III). Additionally, the percentages of larval mortality increased from 28.61% at 5 ppm to 84.69% at 25 ppm after 24 h post-treatment. The overall results of this study point to the potential of *A. articulata* as a substitute biological agent for potential therapeutic/leutic uses in the medical domains and for preventing the proliferation of malarial vector insects.

**Keywords:** biosynthesis; ZnO-NPs; GC-MS; antioxidant; tumor cells; biocontrol; mosquitocidal; *Aedes aegypti*

check for updates

**Citation:** Alamri, A.A.; Alanazi, N.A.H.; Mashlawi, A.M.; Shommo, S.A.M.; Akeel, M.A.; Alhejely, A.; Sulieman, A.M.E.; Salama, S.A. Chemical Composition of *Anabasis articulata*, and Biological Activity of Greenly Synthesized Zinc Oxide Composite Nanoparticles (Zn-NPs): Antioxidant, Anticancer, and Larvicidal Activities. *Agronomy* **2024**, *14*, 1742. https://doi.org/10.3390/agronomy14081742

Academic Editor: Yi Wang

Received: 9 June 2024
Revised: 22 July 2024
Accepted: 6 August 2024
Published: 8 August 2024

**Copyright:** © 2024 by the authors. Licensee MDPI, Basel, Switzerland. This article is an open access article distributed under the terms and conditions of the Creative Commons Attribution (CC BY) license (https://creativecommons.org/licenses/by/4.0/).

## 1. Introduction

Humans have used many Saharan plant species for a variety of uses outside, and not only for treating illness. They have been continuously used by people for therapeutic purposes since the dawn of human life on Earth, and thus they are considered the beginning of the study of plants as potential medicines [1,2]. Numerous types of desert-adapted

medicinal plants, including epiphytes, herbs, and trees, as well as the various plant parts, including roots, barks, leaves, flowers, fruits, and seeds, are regularly used as dietary supplements and as functional foods with the aim of enhancing health in many different countries [3,4]. Plants are a rich source of active phytochemicals, which are crucial for preventing a number of diseases [5].

The *Anabasis* genus (family: Chenopodiaceae) includes 42 plant species distributed in the Mediterranean region and West and Central Asia, where they are grown as medicinal plants and weeds plants. Only four *Anabasis* species have been identified in Egypt's flora, which is heavily grazed by camels and goats and thrives in stony and sandy wadis [6]. *Anabasis* plants contain a variety of secondary metabolites, including triterpenes, glucosidic, flavonoids, saponins, alkaloids, and phenolic chemicals, according to chemical analysis [7–9].

*Anabasis articulata* (Forssk) Moq. is a ubiquitous shrub found in the halic and xeric regions of Egypt. The plant has opposing branches and split-bark stems that can reach a height of 30 cm. It blooms from March to May, with whitish characteristic and dull pinkish solitary flowers [6]. It is a highly beneficial plant that is used in folk medicines in many regions of the world to cure diabetes, headaches, fever, and skin diseases including eczema [10,11]. Moreover, several biological evaluations of the different extracts of *A. articulata* have been documented, including antimicrobial, anti-biofilm, antiulcer, cytotoxic, cholinergic, hepatoprotective, and free radical scavenging activities [7,12–14]. A chemical profile of *A. articulata* aboveground biomass revealed the presence of different secondary metabolites such as triterpenes, saponins, alkaloids and phenolic compounds, fatty acids, and essential oils [7,11,14,15].

Recent research has concentrated on discovering and identifying natural plant compounds as well as the biological uses of extracted plants. When first administered, anticancer medications frequently display potent anticancer effects in drug sensitivity testing or in clinical settings. However, they quickly lead to multidrug resistance and frequently offer no advantages for a patient's life [16]. On the other hand, the Aedes aegypti mosquito is a vector responsible for transmitting various arboviruses including dengue, chikungunya, Zika, and yellow fever. It can be recognized by the white markings on its legs [17]. Sadly, we can now state that efforts to control the *A. aegypti* mosquito population have failed in all tropical regions where the insect is found [18,19]. In order to reduce mosquito populations and disease load, the spread of creative control methods is essential, according to the World Health Organization (WHO) [20]. Synthetic pesticides have negative consequences on the ecosystem, non-target species, and human health as well [21]. The previous studies have examined the effectiveness of ZnO-NPs produced by various wild plants against *A. aegypti*, but the specific application of *A. articulata*-derived ZnO-NPs has not been previously studied.

Zn-ONPs have increased significant attention for their unique properties and applications in biomedicine, catalysis, and environmental remediation [22]. Green synthesis using plant extracts offers an eco-friendly and cost-effective alternative to conventional methods. Successful green synthesis of Zn-ONPs has been reported using various plants, such as *Azadirachta indica*, which showed antimicrobial activity [23], and *Aloe vera*, which demonstrated antioxidant and cytotoxic properties against cancer cell lines [24]. These studies highlight the potential of plant-mediated Zn-ONP synthesis in producing nanoparticles with diverse bioactivities. In this context *A. articulata* extract's chemistry has been studied, and it revealed many biological activities. Allelochemicals, actions against the dengue vector of *A. articulata* extract, and Zn-NPs synthesized using *A. articulata* extract were not previously examined, and little is known about the bioactive components of *A. articulata*. Despite its significance, the plant has not been the subject of many studies. Thus, the objective of the current study will be to (i) employ GC-MS spectroscopy to evaluate the bioactive chemical ingredients of the methanol extract of the Egyptian ecospecies of *A. articulata*, and (ii) in vitro evaluate the antioxidant and cytotoxic activities of the Zn-NPs synthesized using *A. articulata* extract against PC3, MCF-7, and HePG-2 cell lines. Ad-

ditionally, insecticide activity was detected against *A. aegypti* of Zn-NPs fabricated from this species.

## 2. Materials and Methods

### *2.1. Plant Materials Collection and Extraction Process*

Multiple populations of *Anabasis articulata* were collected in April 2022 during the blooming season at Al-Hashr Mountain, Jazan area, Saudi Arabia (17°26′34.80″ N 43° 2′34.79″ E) (Figure 1). In accordance with Tackholm [25] and Boulos [6], the plant was recognized. A voucher specimen (Jaz. 00301010005) was created at Biology Department, Faculty of Science, Jazan University in KSA and added to the herbarium.

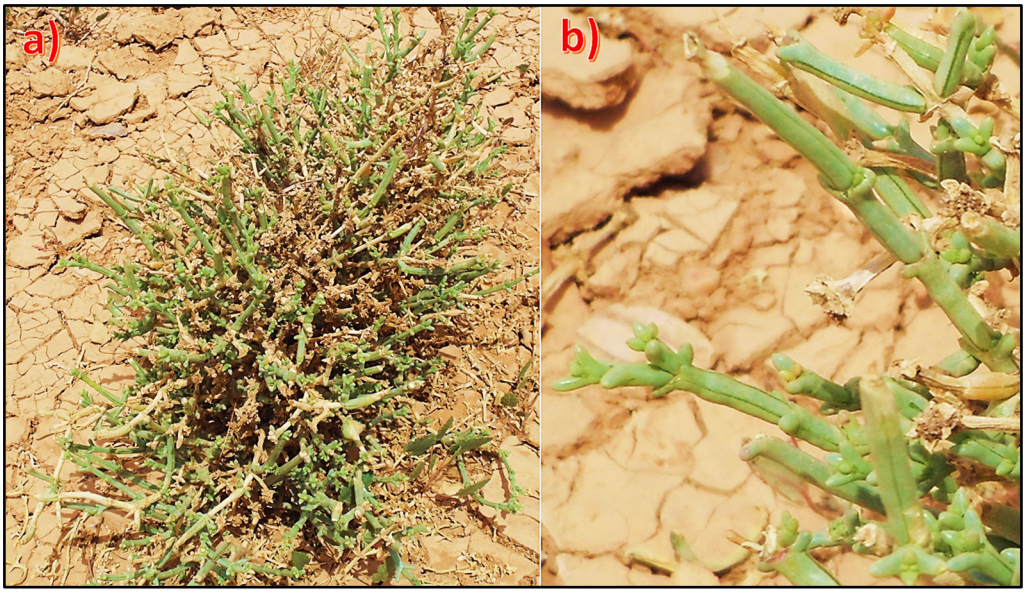



**Figure 1.** *Anabasis articulata* (Forssk) Moq. plant: (**a**) overview of the growing shrub, (**b**) close view of vegetative branch.

The above-ground parts of the plant samples were given time to air dry after washing. A conical flask with a capacity of 250 mL was filled with 10 g of dried plant material and 150 mL of methanol. The mixture was then placed in a water bath shaker (Memmert WB14, Schwabach, Germany), where it was continually stirred for two hours at space temperature. Whatman filter sheets were used to filter the mixture (no. 1, 125 mm, Cat. No. 1012 125, Germany), followed by examining the final plant extract concentrations and keeping the extracts at 4 °C [26].

### *2.2. Characterization of the Chemical Components*

#### 2.2.1. Gas Chromatography–Mass Spectrometry Analysis (GC-MS)

By using the plant extract on a Trace GC-TSQ mass spectrometer (Thermo Scientific, Austin, TX, USA) with a direct capillary column TG-5MS, the bioactive chemical composition of the extracted *A. articulata* plant was reported (30 m × 0.25 mm × 0.25 m film thickness) [27]. The temperature of the column oven was first maintained at 50 °C, then raised by 5 °C per minute to reach 250 °C and maintained for 2 min, and then increased by 30 °C per minute to reach the final temperature of 300 °C and maintained for 2 min. Temperatures of 260 and 270 °C, respectively, were maintained for the transfer line and MS injector. Helium was utilized as the carrier gas with a split ratio of 1:10, and 0.2 µL of the sample was added to the device while being diluted 1:10 in methanol. Plots of the EI mass spectra over the m/z range of 50–500 were made at an ionization voltage of 70 EV. The chemical authentication of the components in the *A. articulata* extract was completed and interpreted by comparing the mass spectra with those of the NIST 14 and WILEY 09 databases.

#### 2.2.2. Phytochemical Analysis

Twenty grams of the dried aerial portions of the plant were combined with 200 mL of deionized water, and agitated for 30 min in a water bath system with a temperature of 70 °C. The extracted product was filtered, and the filtrate was stored for later use at 4 °C. The quantities of phenolics, flavonoids, and tannins were measured in the *A. articulata* aqueous extract.

The total phenolic content was assessed using the Folin–Ciocalteu method established by Wolfe et al. [28] and Issa et al. [29], which utilizes gallic acid (GA) as a standard. The total phenolic content of the aqueous extract of *A. articulata* was determined and converted to milligrams of GA/gram of dry plant extract ($y = 0.00598x$, $r^2 = 0.991$).

The total amount of flavonoids present was determined using a colorimetric assay with aluminum chloride according to Zhishen et al. [30], who utilized catechin as a reference. Using a standard curve ($y = 0.0030x$, $r^2 = 0.981$), the amounts of each flavonoid component were calculated together with the milligram equivalents of catechin per gram of dried plant extract. On the other hand, according to Burlingame [31] and Aberoumand [32], the vanillin–hydrochloride test was used to determine the total quantity of tannins, and tannic acid (TA) equivalents in grams/dried plant per 100 g were given for the expected samples.

### *2.3. Green Synthesis of ZnO-NPs*

The method from Devasenan et al. [33] was used in the production of the metal nanoparticles with a little modification. Briefly, 20 mL of plant extract was added to 20 mL Zinc sulphate (1 mmol). The mixture was agitated for a further two hours at room temperature after the metal aqueous solution had been completely added. Centrifugation was used to collect the generated ZnO-NPs for 15 min at 10,000 rpm. The pellet containing the nanoparticles was kept after centrifugation, while the supernatant was disposed of. Rinsing the obtained ZnO-NPs many times with distilled water ensured that any remaining plant extracts were removed from their surface. Finally, the purified ZnO-NPs were dried at 60 °C for 24 h before being subjected to further characterization.

### *2.4. Structure Characterization of the Metal Nanoparticles*

#### 2.4.1. Transmission Electron Microscope (TEM)

According to Otunola et al. [34], the generated nanoparticles' size, shape, surface type, crystal structure, and morphological details were determined using TEM (JEOL TEM-2200, Tokyo, Japan) at the Electron Microscope Unit, Mansoura University, Egypt. A magnification value of 200 nm was used for this study.

#### 2.4.2. Nanoparticle Characterization Using Zeta Potential

Using the Zeta potential method and Malvern Instruments Ltd., the surface charge of the synthesized ZnNPs in suspension was determined. According to Bhattacharjee [35], the electron microscope unit at Mansoura University in Egypt used Zeta Potential Ver. 2.3 (Kassel, Germany). The procedure was important for understanding how nanoparticle surfaces behave, and it was anticipated that these particles would remain stable over an extended length of time [36].

#### 2.4.3. UV-Vis Spectrophotometer

UV-Vis spectrophotometer was used for recording the UV-Vis spectra of the reaction mixture.

### *2.5. Antioxidant DPPH Assay*

The DPPH (1,1-diphenyl-2 picrylhydrazyl) colorimetric approach was employed in the experiment described by Kitts et al. [37] to assess the antioxidant potency of the methanol extract of *A. articulata* and its zinc nanoparticles. Each sample was prepared for the serial dilution by being combined in an equal quantity with methanol (5, 10, 20, 30, 40, and 50 mg/L). Each concentration of the sample solution was added to the DPPH solution

(1 mL, 0.135 mM). Ascorbic acid concentrations in the analyzed samples were used as the standard. After 30 min at room temperature and in the dark, the samples' absorbance at a wavelength of = 517 nm was determined using a UV-Vis spectrophotometer (Spekol 11 spectrophotometer, analytic Jena AG, Jena, Germany). The percentages of antioxidant scavenging activities were calculated using the following equation, using a DPPH solution in methanol as a reference.

$$\% \text{ Scavenging} = \left[\frac{A_{control} - A_{sample}}{A_{control}}\right] \times 100 \quad (1)$$

The method was used with very few modifications to the earlier experiments [38,39]. The exponential curve [40] that showed the relationship between the sample concentration and the quantity of remaining DPPH• radical was used to calculate the inhibitive concentrations ($IC_{50}$, mg $L^{-1}$).

### *2.6. Cytotoxicity Activity Procedure*

Three unique human tumor cell lines, hepatocellular carcinoma (HePG-2), mammary gland carcinoma (MCF-7), and human prostate cancer (PC3), were donated by the ATCC holding company for biological products and vaccines (VACSERA), Cairo, Egypt. Doxorubicin, a well-known chemotherapeutic anticancer drug, was used as a positive control. Fetal bovine serum (FBS; Gibco Life Technologies, Paisley, UK), MTT, RPMI-1640 medium, and DMSO were the chemical agents utilized (Sigma Co., St. Louis, MO, USA).

#### 2.6.1. Cytotoxicity Assay

To monitor cell growth and evaluate the cytotoxicity of the synthesized Zn-NPs and methanol extract of *A. articulata*, a conventional colorimetric MTT test (2-(4,5-dimethylthiazol2-yl)-3,5-diphenyl-2H-tetrazolium bromide) was conducted according to the instructions provided by Bondock et al. [41]. Briefly, this assay relies on the ability of live cells to convert MTT from yellow to purple formazan crystals via mitochondrial succinate dehydrogenases.

#### 2.6.2. Cell Culture and Treatment

Cell lines were maintained in RPMI-1640 medium and supplemented with 10% FBS and antibiotics (streptomycin 100 µg/mL and penicillin 100 units/mL) in a humidified incubator at 37 °C with 5% $CO_2$. For the cytotoxicity assay, $1.0 \times 10^4$ cells/well were seeded in a 96-well plate and incubated for 48 h. After 24 h, various concentrations of the test samples (including doxorubicin as a positive control) were added to the wells. The experiments were run using seven concentrations (1.56, 3.125, 6.25, 12.5, 25, 50, and 100 µg/mL) prepared in a serial dilution. Following a 24-h incubation with the treatment, MTT solution (5 mg/mL, 20 µL) was added, and the plate was further incubated for 4 h.

#### 2.6.3. Quantification of Cell Viability

A total of 100 µL of DMSO was added to each well to dissolve the formed purple formazan crystals. The absorbance was then measured at 570 nm using a microplate reader (EXL 800, New York, NY, USA). Cell viability was determined based on the absorbance values compared to the control wells (without treatment). The percentage of cell growth inhibition was calculated using the following equation, where OD represents the optical density (absorbance) of the control and treated samples:

$$\% \text{ Inhibition} = \left[\frac{A_{control} - A_{sample}}{A_{control}}\right] \times 100 \quad (2)$$

The $IC_{50}$ values (concentration of the test sample that inhibits cell growth by 50%) were determined using the nonlinear regression (sigmoid type) analysis of the Origin 8.0® software (OriginLab Corporation, https://www.originlab.com; accessed 27 March 2021).

### *2.7. Mosquitocidal Assay*

#### 2.7.1. *Aedes aegypti* Larvae Colony

The *A. aegypti* larvae were supplied by Jizan's Center for Disease Vector and raised for six generations in the Center for Environmental Research, Faculty of Science, Jazan University under precisely regulated conditions of temperature (28 ± 2 °C), relative humidity (70–80%), and 12 light–12 dark cycle. Following their emergence, adult mosquitoes were housed in wooden cages of 30 × 30 × 30 cm for three days, and each day they were fed cotton pieces that had been soaked in a 10.0% sucrose solution. Then, since a blood meal from a pigeon host is required for egg-laying, females were allowed to consume it (anautogeny). A plastic cup oviposition (15 × 15 cm) filled with dechlorinated tap water was placed inside the egg-laying cage. The completed egg rafts were taken out of the plastic dish and put into plastic pans (25 × 30 × 15 cm) with 3 L of tap $H_2O$ that had been sitting for 24 h. The growing larvae were fed one slice of bread every day. The ideal diet for promoting female fertility and larval growth has been shown to be this one [42].

#### 2.7.2. Larvicidal Activity Procedure

The purified nanoparticles were dried and then re-suspended in deionized water to create a stock solution. The toxicity of various biosynthesized ZnO-NP concentrations (25, 20, 15, 10, and 5 mg/mL) was examined against different larval instars (I, II, III, or IV instars) of *A. aegypti*. Briefly, 25 larvae were put into a glass cup together with 500 mL of dechlorinated water, 5 mL of ZnO-NPs (25 mg/mL), and 0.5 mg of the larval meal. Each ZnO-NPs concentration was tested with all larval instars. Each experiment was carried out in conjunction with a ZnO-NPs-free control group [42,43]. Control groups were treated with deionized water alone. The percentages of mortality (%) after 24 h were calculated using the next equation:

$$\% \text{ Larval mortality} = \left[\frac{\text{No.of dead larvae}}{\text{No.of treated larvae}}\right] \times 100 \quad (3)$$

### *2.8. Data Analysis*

The antioxidant and larvicidal activity studies were carried out three times with three replications using the CoStat software, version 6311 (Co.Hort Software, Monterey, CA, USA). The significance of the differences between samples was then determined using a one-way ANOVA on the results.

## 3. Results and Discussion

### *3.1. Gas Chromatography–Mass Spectrometry Analysis (GC-MS)*

The volatile components of the methanol-extracted *Anabasis articulata* were investigated by GC-MS analysis. As shown in Figure 2, the relative abundance of the inspected chemical constitutes was established at a definite retention time. The GC-MS analysis to identify the volatile components was performed with retention after 34.45 min. The chemical constituents based on the GC-MS analysis showed the attending of twenty-six compounds, signifying 100.00% of the total mass (Figure 2 and Table 1). Generally, based on the chemical profile results of *A. articulata*, palmitic acid (fatty acid, 24.48%) was the major abundant component, which was signified after 21.72 min of retention time. The other most volatile components with comparatively good relative abundance were interpreted as (9E,12E)-octadeca-9,12-dienoic acid (10.48%), Stigmast-5-en-3-ol, (3α,24S)- (7.75%), Stigmast-5-en-3-ol, (3α,24R)- (7.61%), methyl (E)-octadec-11-enoate (6.55%), Lup-20(29)-en-3-ol, (3α)- (6.02%), Lup-20(29)-ene-3,28-diol (5.94%), and 6,10,14-trimethylpentadecan-2-one (5.30%). These components were classified as oxygenated hydrocarbon, steroids, fatty acids, and esters of fatty acids. The analysis data indicated the presence of tolerably modest abundant mol of (Z,Z)-1,3-dioctadecenoyl glycerol (3.30%), 1,1,7-trimethyl-4-methylenedecahydro-1H-cyclopropa[e]azulen-7-ol (3.30%), methyl 14-methylpenta-decanoate (2.19%), Estra-1,3,5(10)-trien-17α-ol (2.08%), (2Z,3E)-2-ethylidene-6-methylhepta-3,5-dienal

(1.57%), (E)-2-methyl-4-(2,6,6-trimethylcyclohex-1-en-1-yl)but-2-en-1-ol (1.48%), methyl (9E,12E)-octadeca-9,12-dienoate "Linolelaidic acid, methyl ester" (1.41%), Rhodopin (1.41%), (E)-dec-2-enal (1.31%), 3-ethyl-5-(2-ethylbutyl)octadecane (1.12%), and (E)-3-methyl-2-(pent-2-en-1-yl)cyclopent-2-en-1-one (1.03). Other rare abundant components were documented with a relative abundance lower than 1% (Figure 2).

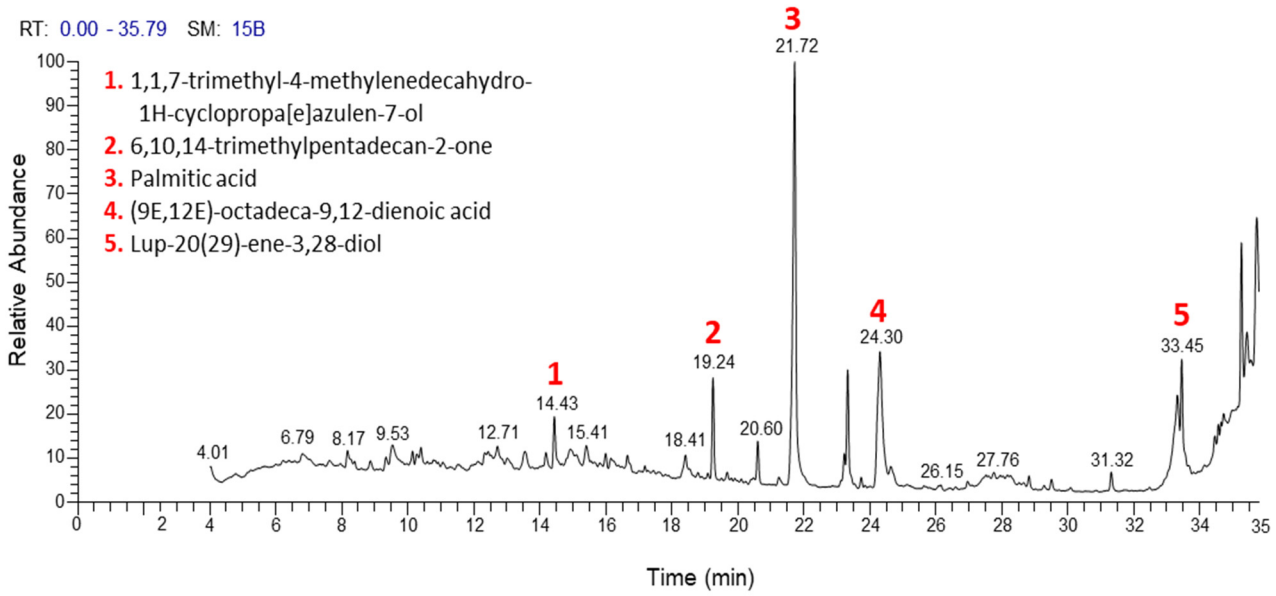



**Figure 2.** Chromatogram and structures of the main components of the MeOH extract of *A. articulata* shoots by GC-MS.

**Table 1.** The characterized chemical components were identified from the extracted shoots of *A. articulata*.

| No. | RT | Chemical Name | Conc. % | Classification | MW | MF |
|---|---|---|---|---|---|---|
| | Hydrocarbons | | | | | |
| 1 | 8.16 | (E)-dec-2-enal | 1.31 ± 0.03 | Oxygenated hydrocarbon | 154.25 | $C_{10}H_{18}O$ |
| 2 | 9.52 | (2Z,3E)-2-ethylidene-6-methylhepta-3,5-dienal | 1.57 ± 0.02 | Oxygenated hydrocarbon | 150.22 | $C_{10}H_{14}O$ |
| 3 | 10.13 | Methyl (E)-2-(prop-1-en-1-yl)-4-(propan-2-ylidene)cyclopentane-1-carboxylate | 0.82 ± 0.01 | Oxygenated hydrocarbon | 208.3 | $C_{13}H_{20}O_2$ |
| 4 | 10.39 | (E)-3-methyl-2-(pent-2-en-1-yl)cyclopent-2-en-1-one | 1.03 ± 0.02 | Oxygenated hydrocarbon | 164.25 | $C_{11}H_{16}O$ |
| 5 | 14.18 | 1-allyl-2,4,5-trimethoxybenzene | 0.97 ± 0.01 | Oxygenated hydrocarbon | 208.26 | $C_{12}H_{16}O_3$ |
| 6 | 15.4 | (E)-2-methyl-4-(2,6,6-trimethylcyclohex-1-en-1-yl)but-2-en-1-ol | 1.48 ± 0.03 | Oxygenated hydrocarbon | 208.35 | $C_{14}H_{24}O$ |
| 7 | 15.99 | Methyl 2-(1-acetyl-5-ethyl-2-(3-(2-hydroxyethyl)-1H-indol-2-yl)piperidin-4-yl)propanoate | 0.84 ± 0.01 | Oxygenated hydrocarbon | 400.52 | $C_{23}H_{32}N_2O_4$ |
| 8 | 16.65 | dotriacontane | 0.85 ± 0.02 | Hydrocarbon | 450.88 | $C_{32}H_{66}$ |
| 9 | 19.24 | 6,10,14-trimethylpentadecan-2-one | 5.30 ± 0.05 | Oxygenated hydrocarbon | 268.49 | $C_{18}H_{36}O$ |
| 10 | 31.32 | 3-ethyl-5-(2-ethylbutyl)octadecane | 1.12 ± 0.02 | Hydrocarbon | 366.72 | $C_{26}H_{54}$ |
| 11 | 34.57 | 2-(3,4-dimethoxyphenyl)-3,5-dihydroxy-7-methoxy-4H-chromen-4-one | 0.78 ± 0.01 | Oxygenated hydrocarbon | 344.32 | $C_{18}H_{16}O_7$ |

**Table 1.** *Cont.*

| No. | RT | Chemical Name | Conc. % | Classification | MW | MF |
|---|---|---|---|---|---|---|
| | Terpenes | | | | | |
| 12 | 14.43 | 1,1,7-trimethyl-4-methylenedecahydro-1H-cyclopropa[e]azulen-7-ol | 3.30 ± 0.04 | Sesquiterpene | 220.36 | $C_{15}H_{24}O$ |
| 13 | 34.72 | Rhodopin | 1.41 ± 0.02 | Tetraterpene | 554 | $C_{40}H_{58}O$ |
| | Steroids | | | | | |
| 14 | 18.41 | Estra-1,3,5(10)-trien-17α-ol | 2.08 ± 0.01 | Steroid | 256 | $C_{18}H_{24}O$ |
| 15 | 33.32 | Lup-20(29)-en-3-ol, (3α)- | 6.02 ± 0.05 | Steroid | 426.73 | $C_{30}H_{50}O$ |
| 16 | 33.45 | Lup-20(29)-ene-3,28-diol | 5.94 ± 0.03 | Steroid | 442.73 | $C_{30}H_{50}O_2$ |
| 17 | 34.45 | Ethyl 3,7,12-trihydroxycholan-24-oate | 0.83 ± 0.01 | Steroid | 436 | $C_{26}H_{44}O_5$ |
| 18 | 35.26 | Stigmast-5-en-3-ol, (3α,24R)- | 7.61 ± 0.06 | Steroid | 414.72 | $C_{29}H_{50}O$ |
| 19 | 35.72 | Stigmast-5-en-3-ol, (3α,24S)- | 7.75 ± 0.08 | Steroid | 414.72 | $C_{29}H_{50}O$ |
| | Fatty acids and esters | | | | | |
| 20 | 20.6 | Methyl 14-methylpentadecanoate | 2.19 ± 0.03 | Ester of fatty acid | 270.46 | $C_{17}H_{34}O_2$ |
| 21 | 21.72 | Palmitic acid | 24.48 ± 0.23 | Fatty acid | 256.43 | $C_{16}H_{32}O_2$ |
| 22 | 23.22 | Methyl (9E,12E)-octadeca-9,12-dienoate "Linolelaidic acid, methyl ester" | 1.41 ± 0.01 | Ester of fatty acid | 294.48 | $C_{19}H_{34}O_2$ |
| 23 | 23.32 | Methyl (E)-octadec-11-enoate | 6.55 ± 0.04 | Ester of fatty acid | 296.5 | $C_{19}H_{36}O_2$ |
| 24 | 24.30 | (9E,12E)-octadeca-9,12-dienoic acid | 10.48 ± 0.05 | Fatty acid | 280.45 | $C_{18}H_{32}O_2$ |
| 25 | 34.64 | Oleic acid, 3-(octadecyloxy)propyl ester | 0.61 ± 0.01 | Ester of fatty acid | 592 | $C_{39}H_{76}O_3$ |
| 26 | 35.43 | (Z,Z)-1,3-dioctadecenoyl glycerol | 3.30 ± 0.04 | Ester of fatty acid | 621 | $C_{39}H_{72}O_5$ |
| Total | | | 100.0 | | | |

RT: Retention time, MW: Molecular weight, MF: Molecular formula.

The wide range of chemical components in *A. articulata* highlights its potential as a rich source of bioactive compounds with diverse biological activities. It is recognized that the current study's findings on the chemical composition of *A. articulata* extracts may vary in terms of the diversity and quantity of components when compared to previous studies. However, research by Mohammed et al. [44] indicated that A. articulata extracts from the Qassim area in Saudi Arabia contained notable levels of palmitic acid (2.09%) and (9E,12E)-octadeca-9,12-dienoic acid (0.71%). Maatalah et al. [45] and Boukhris et al. [46] also identified linoleic acid and stigmast-5-en-3-ol, (3α,24S)- as significant components in Algerian *A. articulata* extracts. Ali et al. [47] similarly noted palmitic acid as a major component in Algerian *A. articulata* extracts. Furthermore, Metwally et al. [13] identified four saponins in the aerial parts of A. articulata from Egypt, including 3-O-glucopyranosyl of (stigmasterol, ß-sitosterol, sitostanol), 3-O-[ß-D glucopyranosyl]oleanolic acid, 3-O-[ß-D-glucopyranosyl-28-O-ß-D-xylopyranosyl] oleanolic acid, and proceric acidin. When estimating the chemical composition of wild plants like *A. articulata*, it is important to consider the influence of genetic factors and various environmental conditions on the production and accumulation of secondary metabolites [48].

The results of the GC-MS analysis have also demonstrated the volatile components as four main classes ascertained as hydrocarbons, including terpenes, steroids, fatty acids, and ester of fatty acids (Table 1). Thus, the major class of these categories is related to the fatty acids and ester (49.02%) of the presented total mass. The order of the other classes is established as follows: steroids (30.23%), hydrocarbons (16.07%), and terpenes (4.71%). Predominantly, eleven components are related to the hydrocarbons, two components are related to terpenes, six components are related to steroids, and seven components are related to fatty acids and esters. The most abundant component for fatty acids class is found to be palmitic acid (24.48%), while Stigmast-5-en-3-ol, (3α,24S)- (7.75%) is the most

abundant molecule between the steroidal types. In addition, 6,10,14-trimethylpentadecan-2-one (5.30%) is the most abundant component as an oxygenated hydrocarbon molecule.

### *3.2. Total Phenolic, Flavonoid, and Tannin Contents*

Biomolecules found in plants, such as proteins, coenzymes, and carbohydrates, have a remarkable capacity to transform metal salts into nanoparticles [49]. The bioactive chemical components of aqueous shoots extract of *A. articulata*, and its sources, include a variety of selected specialized metabolites that have the ability to operate as reducing agents in the biogenic creation of nanoparticles [50]. The current study has shown that the shoot extract of *A. articulata* contains phenolics (189.62 mg GA equivalent/g dry extract), flavonoids (70.16 mg catechin equivalent/g dry extract), and tannins (19.29 mg GA equivalent/g dry extract) that can be used for the stabilization and reduction of zinc metal ions as well as the green synthesis of their nanoparticles. The biological reduction of salt ions into nanoparticles by polyphenol compounds results in an electron resonance hybrid effect. These compounds also play a role in maintaining the nanoparticles in a stable and non-precipitating state.

Several types of nanoparticles (NPs) are produced using a green process, including iron, silver, gold, zinc oxide, and others. Terpenoids and polyphenols, two bioactive components, are found in plant extracts and bio-reduce metallic ions [51]. Phenolics, which may be divided into phenolic acids, flavonoids, and lignin, are significant secondary metabolite chemicals. The bio-reduction of Zn ions into nanoparticles involves the usage of flavonoids, which bind to the surface of the nanoparticles and aggregate to create zero-valent molecules in the nanometer range. Flavonoids are natural chemicals with a variety of phenolic structures that are difficult to break. This leads to the development of novel compounds with extremely tiny sizes, increasing their surface area and enhancing their activity and efficiency [52,53]. Additionally, the amount of phenolics (41.58 mg equivalent GA/g dry extract), flavonoids (16.31 mg equivalent catechin/g dry extract), and tannins (5.34 mg equivalent GA/g dry extract) in the nano zinc generated was greatly reduced (Table 2).

**Table 2.** The phytochemical analysis of the investigated extracted samples.

| Samples | Phytochemical Analysis | | |
|---|---|---|---|
| | **Phenolics Content** | **Flavonoids Content** | **Tannins Content** |
| *Anabasis articulata* | 189.62 | 70.16 | 19.29 |
| *Anabasis articulata*-ZnNPs | 41.58 | 16.31 | 5.34 |

Phenolics Content "mg gallic acid/1 gm dry extract", Flavonoids Content "mg catechin/1 gm dry extract" and Tannins Content "mg tannic acid/1 gm dry extract".

### *3.3. Characterization of the Prepared Nanoparticles*

#### 3.3.1. UV-Visible Spectrophotometer

The optical characteristics of the produced ZnO-NPs solution were examined using a UV-Vis spectrophotometer with a scan range of 190 to 850 nm. In Figure 3, the spectrum of the purified ZnO nanoparticles displays a distinct absorption peak at 283 nm. This peak was absent in the spectra of both the plant extract and the reaction mixture. Moreover, the UV-Vis spectra of the plant extract showed a maximum absorption peak at a wavelength of 245 nm with an absorbance of 0.873. The results showed that the highest ZnO-NPs absorbance readings were obtained at 246 nm, which suggested that the corresponding nanoparticles had formed in the solution and was verified as a sign in Figure 3. The investigated ZnO-NPs solutions' absorption spectra showed a blue shift. Depending on the sample concentration, energy, light speed, and wavelength, this behavior is consistent with earlier findings [54]. The findings made it abundantly evident that the extract of *A. articu-lata* effectively reduced zinc ions.

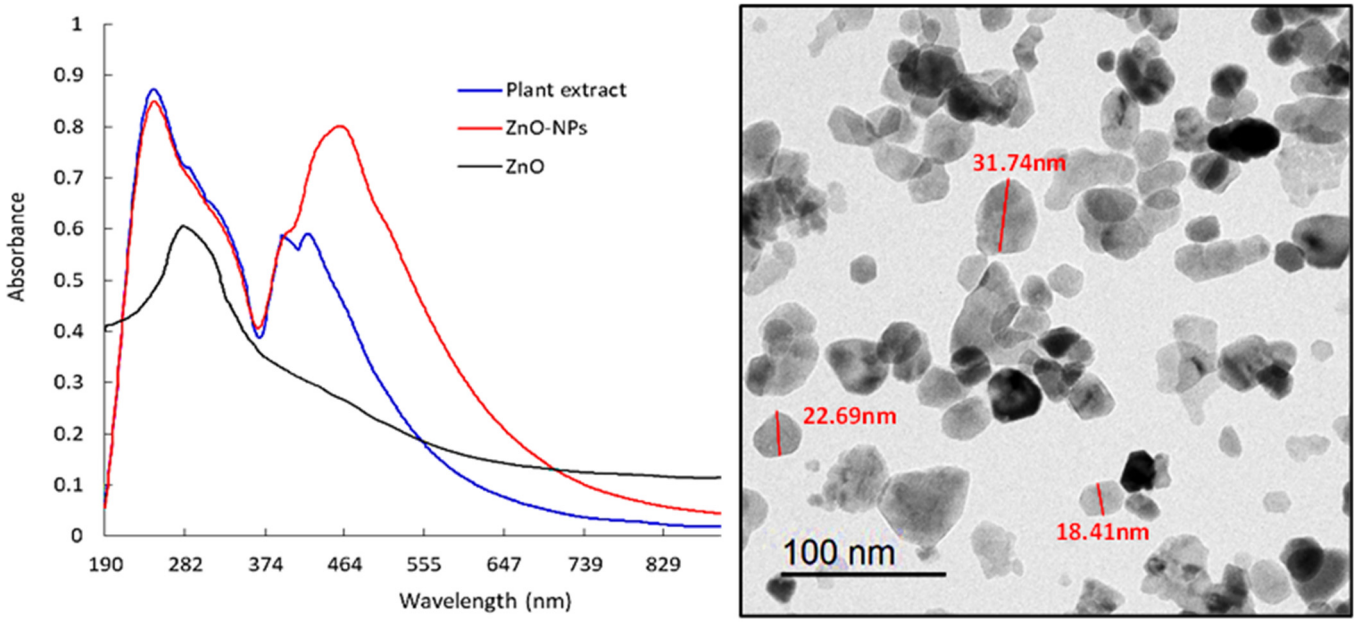



**Figure 3.** The UV-visible spectroscopy graphs of the plant extract, ZnO and prepared ZnO-NPs, and TEM configurations of ZnNPs.

### 3.3.2. Transmission Electron Microscope (TEM)

The crystallography and size dimension of the nanoparticles prepared using *A. articulata* plant extract were intuitively obtained from the TEM image (Figure 3). The analyses of the samples were run on TEM (JEOL TEM-2100, Tokyo, Japan) with 200 nm of magnification at the Electron Microscope Unit, Central Laboratory, Mansoura University. The TEM images of the produced zinc nanoparticles are shown in Figure 3. The collected data indicated a decreased size of less than 100 nm given the nanoparticle size. In the case of zinc, the nanoparticles are spherical, trigonal, and tetragonal in form. Regardless, spherical forms provide a greater surface area with a better influence on the resolution of the biological impacts. The nanoparticles are also more aggregated, and the aggregation factor influences the solution's effectiveness for better biological outcomes [34].

### 3.3.3. Zeta Potential Analysis

Zeta potential analysis was performed on Malvern Instruments Ltd., Zeta Potential Ver. 2.3 (Kassel, Germany) to assess the stability of the synthesized nanoparticles. Bhattacharjee et al. [35] reported that nanoparticles with Zeta potential values above +30 mV or below −30 mV are considered highly stable. In this study, the Zeta potential value of the nanoparticles synthesized using *A. articulata* extract was −0.324 mV. While this value suggests limited stability according to the classification, other factors like steric hindrance due to capping agents present in the extract might also contribute to the overall stability of the nanoparticles. Further investigations, such as monitoring aggregation over time, could provide more insights into the long-term stability of the nanoparticles (Figure 4).

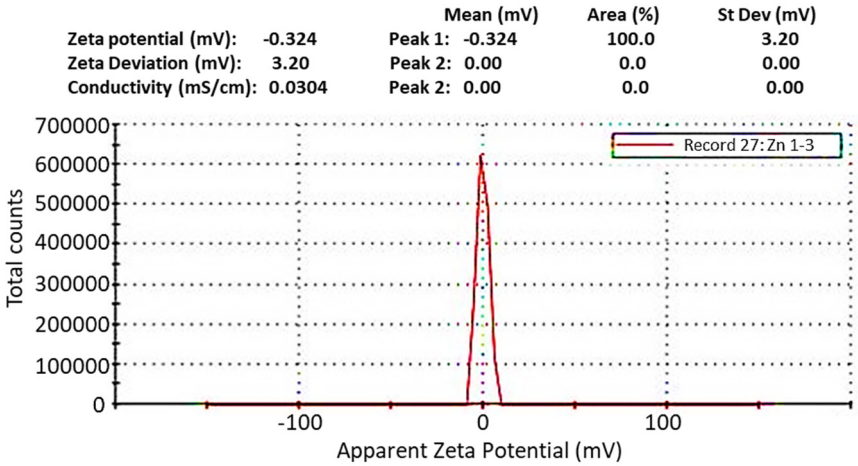



**Figure 4.** Zeta potential analysis of ZnNPs.

### *3.4. Biological Characteristics of the Plant Extracts*

#### 3.4.1. Antioxidant Activity—DPPH Assay

The ability of the *A. articulata* extract to trap DPPH free radicals in the solution via a free radical pathway is known as its antioxidant capability. In the present study, the plant extract has a superior activity for trapping the free radicals of DPPH in the solution to the metal nanoparticle solutions, according to comparisons of the tested samples' findings with those of ascorbic acid. The results mostly concur with phytochemical findings because the sample may more effectively trap free radicals in the solution because of its phenolic concentration. At a concentration of 50 mg/mL, *A. articulata* extract demonstrated 73.64% of percent scavenging activity; this result is comparable to ascorbic acid (67.91% at 20 mg/mL). Although the generated ZnNPs (44.63%) solutions' findings for scavenging activity percentages seemed to be lower than those for the plant extract, all samples showing an increase in the activity by increasing the sample concentration revealed proportional correlations (Table 3).

**Table 3.** The antioxidant results (% scavenging activity, and $IC_{50}$ (mg/mL)) of the investigated extracted samples.

| Concentrations (mg/mL) | % Scavenging Activity | |
|---|---|---|
| | ***A. articulata*** | ***A. articulata*-ZnNPs** |
| 50 | 73.64 ± 1.56 | 44.63 ± 1.36 |
| 40 | 61.52 ± 1.37 | 33.17 ± 1.32 |
| 30 | 53.02 ± 1.91 | 26.55 ± 1.14 |
| 20 | 45.52 ± 1.35 | 18.72 ± 0.98 |
| 10 | 34.16 ± 1.28 | 8.88 ± 0.54 |
| 5 | 23.24 ± 1.08 | 6.48 ± 0.28 |
| $IC_{50}$ (mg/mL) | 27.48 | 69.53 |
| F-value | 2.04 *** | 1.67 *** |
| | Ascorbic acid | |
| 20 | 67.91 ± 1.27 | |
| 15 | 57.96 ± 0.89 | |
| 10 | 46.71 ± 0.71 | |
| 5 | 39.88 ± 0.56 | |
| 2.5 | 8.27 ± 0.06 | |
| 1 | 2.64 ± 0.03 | |
| $IC_{50}$ (mg/mL) | 12.78 | |
| F-value | 1.40 *** | |

Values significance at probability level of 0.001 (*** $p < 0.001$).

An increased ability to scavenge DPPH radicals is shown by a decreased $IC_{50}$ value. The A. articulata shoot extract had the highest antioxidant scavenging activity with an $IC_{50}$ value of 27.48 mg/mL compared to the ascorbic acid's result (12.78 mg/mL), according to the data shown in Table 2. The lowering of the antioxidant scavenging activity with $IC_{50}$ = 69.53 mg/mL was obviously caused by the creation of metal nanoparticles ZnNPs by the action of the *A. articulata* extract. The availability of oxygen sources such as fatty acids, phenolic compounds, oxygenated hydrocarbons, and esters of fatty acids to trap the free radicals of DPPH in the solution was the mechanism of this antioxidant process. Palmitic acid, (9E,12E)-octadeca-9,12-dienoic acid; stigmast-5-en-3-ol, (3α,24S)-; methyl (E)-octadec-11-enoate; Lup-20(29)-en-3-ol, (3α)-; Lup-20(29)-ene-3,28-diol and 6,10,14-trimethylpentadecan-2-one are the main volatile components of this plant extract, and they have the potential to stop free radical reactions [55–57].

In contrast, fatty acids and lipids extracted from *Sisymbrium irio*, *Aesculus indica*, and *Rumex vesicarius* exhibited potent antioxidant capabilities by scavenging free radicals in the solution [58,59]. Reactive oxygen species, such as fatty acids, terpenes, oxygenated hydrocarbons, and carbohydrates, are widely used as proxies for free radicals to measure the antioxidant capability of bioactive compounds [38,60]. In addition, the antioxidant activity of *A. articulata* shoot extract was equivalent to that of the methanolic extract of the species' stems, with an $IC_{50}$ inhibitory concentration of 24.01 mg/mL [61]. Furthermore, *A. articulata* shoot extract showed antioxidant properties on par with *Origanum vulgare* from the Mediterranean region, known for its high phenolic content and strong antioxidant activity [62]. The capacity of plants to defend themselves against free radicals has been demonstrated to be inversely proportional to the concentration of bioactive substances, particularly phenolic components such as flavonoids, phenolic acids, ascorbic acid, and carotenoids [14,63]. According to our findings, this plant contains a variety of nonvolatile chemicals such as tannins, flavonoids, and phenols.

#### 3.4.2. Anticancer Activity

The cytotoxic activity was assessed for the extracted *A. articulata* and its ZnO-NPs solutions by applying MTT assay against the different tumor and normal cell lines. In the present results, the cytotoxic activity evaluations were conducted for *A. articulata* extracts against the three cancer cell lines, i.e., hepatocellular carcinoma (HePG-2), human prostate cancer (PC3), and mammary gland carcinoma (MCF-7) (Table 4). Human lung fibroblast cell lines (WI-38) were also used to test the extracts for toxicity in a laboratory setting. Doxorubicin was selected as a standard medicine against which other treatments may be compared. The $IC_{50}$ values are the doses in µg /mL that cause 50% of the tumor cells to die. The effectiveness of the sample at slowing the proliferation of cancer cells is negatively correlated with the $IC_{50}$ values. Therefore, the lowest concentration and $IC_{50}$ values would be needed for a powerful cytotoxic agent.

**Table 4.** Cytotoxic activity of the prepared samples against the studied tumor and normal cell lines.

| Samples | In Vitro Cytotoxicity, $IC_{50} \pm$ SD (µg/mL) | | | |
|---|---|---|---|---|
| | **HePG-2** | **MCF-7** | **PC3** | **WI-38** |
| Doxorubicin | 5.06 ± 0.31 | 4.26 ± 0.28 | 8.09 ± 0.32 | 96.54 |
| *A. articulata* | 40.34 ± 2.98 | 49.62 ± 3.01 | 60.51 ± 3.21 | >100 |
| *A. articulata* + ZnNPs | 21.19 ± 1.20 | 30.91 ± 2.07 | 49.32 ± 2.88 | >100 |
| Zinc sulfate | 56.1 ± 2.65 | 68.67 ± 3.42 | 72.61 ± 3.91 | >100 |

$IC_{50}$: inhibitory concentration. (µg): 1–10 (very strong), 11–20 (strong), 21–50 (moderate), 51–100 (weak), and above 100 (non-cytotoxic).

Table 4 includes a list of the in vitro cytotoxicity data together with information on the samples' levels of cell viability or potency. The outcomes showed that, in comparison to the original extract, the produced zinc nanoparticles displayed stronger cytotoxicity against a variety of tumor cell types. Consequently, the nanoparticles' large surface area improved

the sample's ability to stunt the development of tumor cells. Furthermore, the $IC_{50}$ value for cytotoxicity against HePG-2 cell lines was 21.19 µg/mL, which was found in *A. articulata's* zinc nanoparticles. Additionally, $IC_{50}$ values for *A. articulata* zinc nanoparticles against MCF-7 and PC3 tumor cell lines were 30.91 and 49.32 µg/mL, respectively, indicating considerable cytotoxicity. The $IC_{50}$ values of the examined *A. articulata* extract samples showed the maximum cytotoxic activity against the HePG-2 at 40.34 µg/mL, followed by the MCF-7 ($IC_{50}$ = 49.62 µg/mL) and the PC3 ($IC_{50}$ = 60.51 µg/mL) (Table 4). The cytotoxic effects of the tested samples on three tumor cell lines were dose-dependent (Figure 5). Moreover, the $IC_{50}$ values for all the samples showed that they were safe to use around normal human lung fibro-blast cells (WI-38) (i.e., weak cytotoxic activities). The results raised the possibility that the samples may be utilized to create anticancer medications. Whether tested as a basic extract or for its separated zinc nanoparticles, *A. articulata* showed promising cytotoxic activity against all of the tested tumor cell lines. Furthermore, the results of the examined salt solutions demonstrated the efficacy of the isolated *A. articulata*, and its zinc nanoparticles on the cytotoxicity demonstrated very mild cytotoxicity against HePG-2, MCF-7, and PC3 tumor cell lines. In simple terms, the cytotoxicity against the various evaluated tumor cell lines was not affected by the salts.

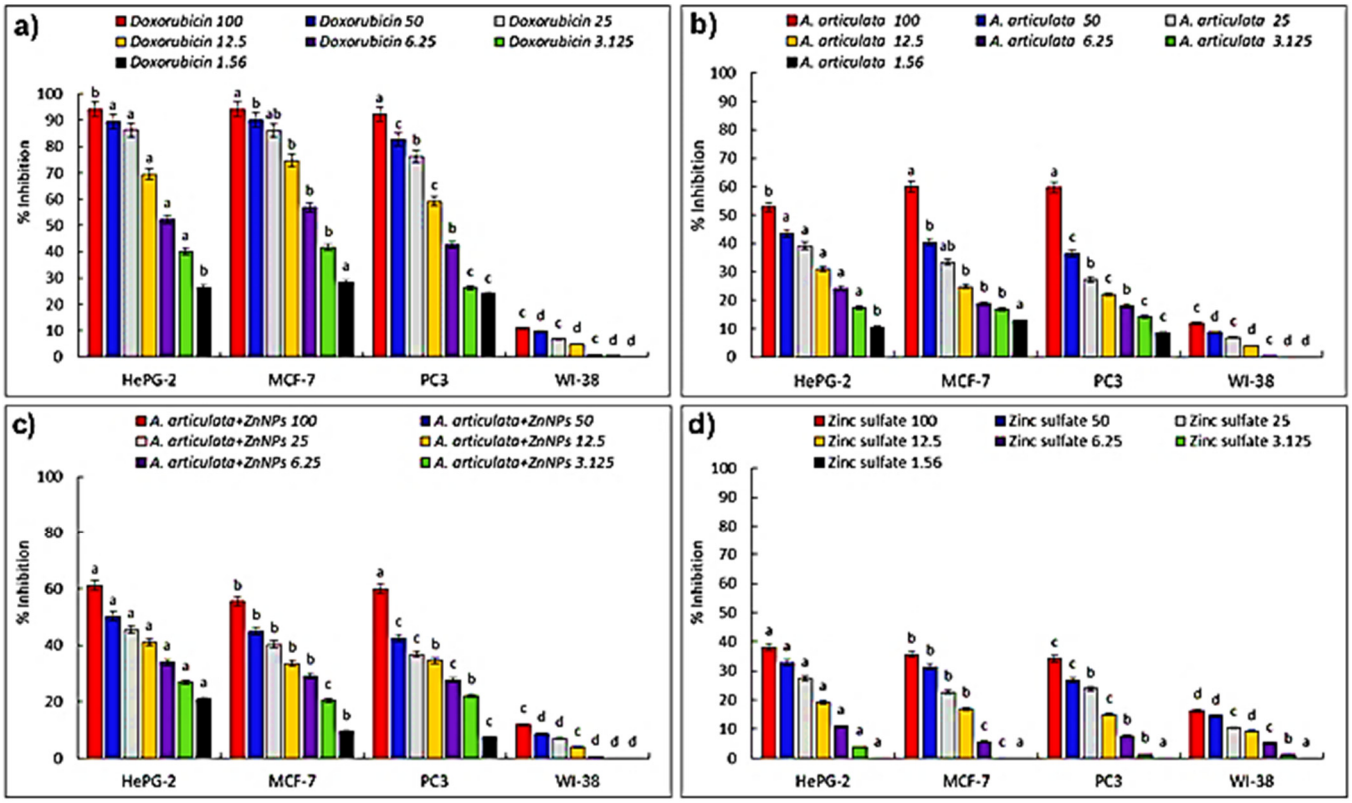



**Figure 5.** Comparison of the inhibition percentage of tumor and normal cells at different concentrations. Locations: (**a**) for doxorubicin, (**b**) for *A. articulata* extract, (**c**) for *A. articulata* + ZnNPs, and (**d**) for zinc sulfate solution. Different superscript letters within each treatment express significant variation at a probability level of 0.05 (Duncan's test).

Table 4 shows a comparison of the outcomes of the *A. articulata* extract and its zinc nanoparticles against HepG-2, MCF-7, and PC3 cell lines with the results of doxorubicin. Drugs were also shown to have high cytotoxicity against HepG-2, MCF-7, and PC3 cell lines ($IC_{50}$ = 5.06, 4.26, and 8.09 µg/mL, respectively). It is worth noting that the addition of metal nanoparticles to the *A. articulata* extract boosted its cytotoxic effects to varied degrees. The nature of the metal in the nanoparticles used, which were characterized

as having microscopic particles and enhanced aggregation, determined whether the zinc nanoparticles or the extract of *A. articulata* itself generated different results.

Figure 5 displays the percentage of human tumor cells that the A. articulata extract and its metal nanoparticles were able to inhibit at various doses. The samples were created by a series of seven concentration dilutions commencing at 1.56 µg/mL. The findings showed that using a sample at a greater concentration boosted the sample's ability to inhibit the growth of cancer cells. As a result, the *A. articulata* extract revealed strong cytotoxicity with inhibition percentages ranging from 52.77% to 59.94% at a dosage of 100 µg/mL, whereas 1.56 µg/mL of the same *A. articulata* extract had no effect on any of the cancer cell lines that were examined. Results from the addition of zinc nanoparticles to the extracted *A. articulata* showed that the nanoparticles could enhance the extract's anticancer activity against all the cancer cell lines that had been evaluated. Additionally, the zinc sulphate solutions at various doses (1.56–100 µg/mL) had their percent of inhibition determined. The zinc sulphate solution's percentage of inhibition against various tumor cell lines ranged from 34.2% to 38.1% as the metal salt demonstrated moderate activities at higher doses (100 µg/mL). According to observations in the literature [54,55,58,64,65], metal nanoparticle solutions have significant cytotoxic properties against the development of tumor cell types.

In the last few years, reports demonstrating the use of ZnO-NPs for the delivery of chemotherapeutic drugs to treat cancer have proliferated [66,67]. The size of ZnO-NPs has been reported to have a strong association with their anticancer activities. According to the literature, nano-zinc may be stabilized by encapsulating it in appropriate nano-vehicles and exhibits decreased toxicity and excellent bioavailability in its zero-oxidation form [68]. Due to its distinct physical characteristics, biocompatible nanosized zinc oxide (ZnO) has achieved significant scientific advancements. Since $Zn^{2+}$ is a necessary nutrient for adults, ZnO nanoparticles are being developed and are thought to be safe in vivo. These advantages make ZnO-NPs an excellent choice for biocompatible and biodegradable nano-platforms, and they can also be examined for use in the treatment of cancer [69,70]. Recently, the ZnO-NPs have received a lot of interest because of their distinct antibacterial activity and application as drug delivery vehicles. The ZnO-NPs are said to help in medication distribution, have conductive coating activity, and are generally biocompatible [71].

#### 3.4.3. Larvicidal Bioassay

The majority of people immediately link malaria to mosquitoes. However, a variety of other illnesses can also be spread by these small flying insects. The world's health and socioeconomic stability are seriously threatened by new viral vectors from the *Aedes* mosquito species [72]. The most well-known *Aedes*-borne viruses are dengue virus (DENV), yellow fever virus (YFV), chikungunya virus (CHIKV), and zika virus (ZIKV), due to the size of the outbreaks they create and the severity of the illnesses they cause [55,73]. The results of this study demonstrated a substantial increase in larval mortality at all doses of *A. articulata* extract. There was no larval death when the concentration was determined to be 5 ppm for 24 h, compared to 1.66% for the control group; however, the largest larval mortality (38.42%) was recorded at a concentration of 25 ppm for 24 h.

In this study, the effectiveness of biosynthesized ZnO-NPs as larvicidal agents against *A. aegypti* was examined. Data analysis revealed that ZgO-NPs' larvicidal potential was dose- and time-dependent. The percentages of larval mortality increased from 28.61% at 5 ppm to 84.69% at 25 ppm, according to the data shown in Table 5. In addition, the $LC_{50}$ (the concentration of ZnO-NPs that causes 50% mortality) and $LC_{90}$ (the concentration of ZnO-NPs that causes 90% mortality) for the III instar were 13.64 ppm and 26.23 ppm, respectively.

**Table 5.** The toxicity of biosynthesized ZnO-NPs against 3rd larval instar of *Aedes aegypti* larvae.

| Conc. (mg/L) | Mortality Percentages (%) after 24 h Post-Treatment | |
|---|---|---|
| | Plant Extract | ZnO-NPs |
| 5 | 0.00 $^{D}$ | 28.61 ± 0.86 $^{E}$ |
| 10 | 17.20 ± 1.02 $^{C}$ | 39.73 ± 1.01 $^{D}$ |
| 15 | 24.04 ± 1.31 $^{B}$ | 52.08 ± 1.84 $^{C}$ |
| 20 | 34.21 ± 1.68 $^{A}$ | 71.43 ± 2.23 $^{B}$ |
| 25 | 38.42 ± 1.48 $^{A}$ | 84.69 ± 2.65 $^{A}$ |
| Control | 1.66 ± 0.3 $^{D}$ | 1.66 ± 0.31 $^{F}$ |
| *F-value* | 733.20 | 523.63 |
| *p-value* | <0.0001 *** | <0.0001 *** |
| $LC_{50}$ | 32.08 | 13.64 |
| $LC_{90}$ | 59.36 | 26.23 |

Mortality was expressed as mean ± SE (standard error) of 3 replicates. Different superscript letters within each treatment (column) express significant variation at a probability level of 0.05 (Duncan's test). *** $p < 0.001$.

The effectiveness of nanoparticles against several mosquito species has already been studied. Manimaran et al. [74] discovered that *Lobelia leschenaultiana*-mediated ZnO-NPs were particularly efficient against the *Aedes aegypti* mosquito vector. With an $LC_{50}$ of 1.57 mg/L, ZnO-NPs (at 10 mg/mL) displayed the highest percentage larval death of 100%. Patil et al. [75] found that AgNP derived from *Pergularia daemia* latex was poisonous to *A. aegypti* and *A. stephensi* larvae (III), with $LC_{50}$ values of 5.66 mg/L and 5.91 mg/L, respectively. The $LC_{50}$ of *Annona muricata*-produced AgNP was effective against a variety of mosquito vectors, including *A. aegypti* (12.58 g/mL), *A. stephensi* (15.28 mg/L), and *C. quinquefasciatus* (18.77 mg/L) [76]. Gold nanoparticles produced by *Cymbopogon citratus* were tested against third-instar *A. stephensi* and *A. aegypti* larvae, with $LC_{50}$ values of 25.92 and 8.63 mg/mL, respectively [77]. Furthermore, the $LC_{50}$ values of $TiO_2$-NPs produced by *Argemone mexicana* against *A. aegypti* larvae (III) were 26.1 mg/L and 56.5 mg/L (III) [78]. When the acquired data were compared to earlier research, it was possible to infer that the biosynthesized ZnO-NPs were more harmful to various instar larvae at low concentrations. The promising results suggest that *A. articulata* could serve as a valuable source for developing effective mosquito repellents.

## 4. Conclusions

In conclusion, twenty-six compounds, signifying 100.00% of the total mass, were identified based on the chemical profile results of *A. articulata* aerial parts. Palmitic acid (fatty acid, 24.48%) is the major abundant component. The other most volatile components with comparatively good relative abundance were interpreted as (9E,12E)-octadeca-9,12-dienoic acid (10.48%), Stigmast-5-en-3-ol, (3α,24S)-(7.75%), and Stigmast-5-en-3-ol, (3α,24R)-(7.61%). The ZnO-NPs were effectively produced from *A. articulata* in the present work. UV-Vis, TEM, and Zeta potential analyses were used to characterize them as formed ZnO-NPs. The peak of ZnO-NPs at 246 nm was confirmed by UV-Vis spectral analysis. The findings of the particle size study represented the average size distribution of ZnO-NPs (24.38 nm). The characterization of these nanoparticles showed that they have a substantial negative Zeta potential, indicating good stability in suspension. Zinc nanoparticles displayed improved stability and a range of acceptable morphologies due to the presence of specific chemical components, such as phenolics, flavonoids, tannins, and alkaloids content, which were responsible for nanoparticle formation and stability. Biosynthesized ZnO-NPs' biological activity were shown to be time- and concentration-dependent. The biogenic ZnO-NPs demonstrated strong larvicidal and anticancer effects, as well as diminished antioxidant capabilities, at low doses. The nano-zinc solution of the plant extract produced the strongest cytotoxic effects against HePG-2 cell lines, with an $IC_{50}$ of 21.19 µg/mL. *A. articulata* zinc nanoparticles also showed moderate cytotoxicity, with $IC_{50}$ values of 30.91 and 49.32 µg/mL against MCF-7 and PC3 tumor cell lines, respectively. *Aedes aegypti* instar (III) had $LC_{50}$ and

$LC_{90}$ values of 13.64 and 26.23 mg/L, respectively. Additionally, the antioxidant properties and phytochemical constituents were found to be much lower than in the original extract. These findings highlight the promising applications of A. articulata-derived ZnO-NPs in controlling disease vectors and cancer.

**Author Contributions:** Conceptualization, A.A.A., N.A.H.A., A.M.M., S.A.M.S., M.A.A., A.A., A.M.E.S. and S.A.S.; formal analysis, A.A.A., N.A.H.A., A.M.M., S.A.M.S., M.A.A., A.A., A.M.E.S. and S.A.S.; investigation, A.A.A., N.A.H.A., A.M.M., S.A.M.S., M.A.A., A.A., A.M.E.S. and S.A.S.; data curation, A.A.A., N.A.H.A., A.M.M., S.A.M.S., M.A.A., A.A., A.M.E.S. and S.A.S.; writing—original draft preparation, A.A.A., N.A.H.A., A.M.M., S.A.M.S., M.A.A., A.A., A.M.E.S. and S.A.S.; writing—review and editing, A.A.A., N.A.H.A., A.M.M., S.A.M.S., M.A.A., A.A., A.M.E.S. and S.A.S. All authors have read and agreed to the published version of the manuscript.

**Funding:** This work was supported by the Scientific Research Deanship at the University of Ha'il in Saudi Arabia (RG-23 217), which provided funding.

**Data Availability Statement:** The data presented in this study are available upon request from the corresponding author.

**Acknowledgments:** The authors extend their appreciation to the Scientific Research Deanship at the University of Ha'il in Saudi Arabia for funding this research work through Project Number RG-23 217.

**Conflicts of Interest:** The authors declare no conflicts of interest.

## References

1. McGaw, L.J.; Famuyide, I.M.; Khunoana, E.T.; Aremu, A.O. Ethnoveterinary botanical medicine in South Africa: A review of research from the last decade (2009 to 2019). *J. Ethnopharmacol.* **2020**, *257*, 112864. [CrossRef] [PubMed]
2. Muthu, C.; Ayyanar, M.; Raja, N.; Ignacimuthu, S. Medicinal plants used by traditional healers in Kancheepuram District of Tamil Nadu, India. *J. Ethnobiol. Ethnomed.* **2006**, *2*, 43. [CrossRef] [PubMed]
3. Shi, J.; Ho, C.-T.; Shahidi, F. *Functional Foods of the East*; CRC Press: Boca Raton, FL, USA, 2011.
4. Muimba-Kankolongo, A.; Ng'andwe, P.; Mwitwa, J.; Banda, M.K. Non-Wood Forest Products, Markets, and Trade. In *Forest Policy, Economics, and Markets in Zambia*; Elsevier: Amsterdam, The Netherlands, 2015; pp. 67–104.
5. Lim, T.K. *Edible Medicinal and Non-Medicinal Plants*; Springer: Dordrecht, The Netherlands, 2012; Volume 1.
6. Boulos, L. *Flora of Egypt*; Al Hadara Publishing: Cairo, Egypt, 1999.
7. Gamal, G.; Abo-El-Seoud, K.A.; Attia, G. Triterpenoids from the aerial parts of *Anabasis articulata* (Forssk) Moq: Gastroprotective effect in vivo with in silico studies, cytotoxic and antimicrobial activities. *Nat. Prod. Res.* **2021**, *36*, 4076–4084. [CrossRef] [PubMed]
8. Chen, H.; Hajia, A.; Yang, Z.; Li, Y. Isolation and structure identification of chemical constituents from Anabasis brevifolia. *Yao Xue Xue Bao = Acta Pharm. Sin.* **2005**, *40*, 248–251.
9. Kambouche, N.; Merah, B.; Derdour, A.; Bellahouel, S.; Younos, C.; Soulimani, R. Activité antihyperglycémiante d'un stérol β-sitoglucoside isolé de la plante *Anabasis articulata* (Forssk) Moq. *Phytothérapie* **2011**, *9*, 2–6. [CrossRef]
10. Hammiche, V.; Maiza, K. Traditional medicine in Central Sahara: Pharmacopoeia of Tassili N'ajjer. *J. Ethnopharmacol.* **2006**, *105*, 358–367. [CrossRef] [PubMed]
11. Kambouche, N.; Merah, B.; Derdour, A.; Bellahouel, S.; Bouayed, J.; Dicko, A.; Younos, C.; Soulimani, R. Hypoglycemic and antihyperglycemic effects of *Anabasis articulata* (Forssk) Moq (Chenopodiaceae), an Algerian medicinal plant. *Afr. J. Biotechnol.* **2009**, *8*, 5589–5594.
12. Al-Joufi, F.A.; Jan, M.; Zahoor, M.; Nazir, N.; Naz, S.; Talha, M.; Sadiq, A.; Nawaz, A.; Khan, F.A. *Anabasis articulata* (Forssk.) Moq: A Good Source of Phytochemicals with Antibacterial, Antioxidant, and Antidiabetic Potential. *Molecules* **2022**, *27*, 3526. [CrossRef] [PubMed]
13. Metwally, N.S.; Mohamed, A.M.; ELSharabasy, F.S. Chemical constituents of the Egyptian Plant *Anabasis articulata* (Forssk) Moq and its antidiabetic effects on rats with streptozotocin-induced diabetic hepatopathy. *J. Appl. Pharm. Sci.* **2012**, *2*, 54–65. [CrossRef]
14. Benhammou, N.; Ghambaza, N.; Benabdelkader, S.; Atik-Bekkara, F.; Panovska, F.K. Phytochemicals and antioxidant properties of extracts from the root and stems of *Anabasis articulata*. *Int. Food Res. J.* **2013**, *20*, 2057.
15. Segal, R.; Goldzweig-Milo, I.; Zaitschek, D. sapogenin content of *Anabasis articulata*. *Phytochemistry* **1969**, *8*, 521–526. [CrossRef]
16. Krishna, R.; Mayer, L.D. Multidrug resistance (MDR) in cancer: Mechanisms, reversal using modulators of MDR and the role of MDR modulators in influencing the pharmacokinetics of anticancer drugs. *Eur. J. Pharm. Sci.* **2000**, *11*, 265–283. [CrossRef] [PubMed]
17. Sukhralia, S.; Verma, M.; Gopirajan, S.; Dhanaraj, P.; Lal, R.; Mehla, N.; Kant, C.R. From dengue to Zika: The wide spread of mosquito-borne arboviruses. *Eur. J. Clin. Microbiol. Infect. Dis.* **2019**, *38*, 3–14. [CrossRef] [PubMed]
18. Plourde, A.R.; Bloch, E.M. A literature review of Zika virus. *Emerg. Infect. Dis.* **2016**, *22*, 1185. [CrossRef]

19. Mendez-Sanchez, S.; Chaverra-Rodriguez, D.; Duque, J. Aedes aegypti and the use of natural molecules for its control: Implications in the decrease of Zika disease. In *Zika Virus Impact, Diagnosis, Control, and Models*; Elsevier: Amsterdam, The Netherlands, 2021; pp. 317–325.
20. Jones, R.T.; Ant, T.H.; Cameron, M.M.; Logan, J.G. Novel Control Strategies for Mosquito-Borne Diseases. *Philos. Trans. R. Soc.* **2021**, *376*, 20190802. [CrossRef] [PubMed]
21. Weeratunga, P.; Rodrigo, C.; Fernando, S.D.; Rajapakse, S. Control methods for Aedes albopictus and Aedes aegypti. *Cochrane Database Syst. Rev.* **2017**, *8*, CD012759.
22. Raj, V.J.; Ghosh, R.; Girigoswami, A.; Girigoswami, K. Application of zinc oxide nanoflowers in environmental and biomedical science. *BBA Adv.* **2022**, *2*, 100051. [CrossRef]
23. Sangeetha, G.; Rajeshwari, S.; Venckatesh, R. Green synthesis of zinc oxide nanoparticles by aloe barbadensis miller leaf extract: Structure and optical properties. *Mater. Res. Bull.* **2011**, *46*, 2560–2566. [CrossRef]
24. Mahendiran, D.; Subash, G.; Arumai Selvan, D.; Rehana, D.; Senthil Kumar, R.; Kalilur Rahiman, A. Biosynthesis of zinc oxide nanoparticles using plant extracts of Aloe vera and Hibiscus sabdariffa: Phytochemical, antibacterial, antioxidant and anti-proliferative studies. *BioNanoScience* **2017**, *7*, 530–545. [CrossRef]
25. Tackholm, V. *Students' Flora of Egypt*; Cairo University Publishing: Giza, Egypt, 1974.
26. Souza, M.M.; Silva, B.D.; Costa, C.S.; Badiale-Furlong, E. Free phenolic compounds extraction from Brazilian halophytes, soybean and rice bran by ultrasound-assisted and orbital shaker methods. *An. Acad. Bras. Ciências* **2018**, *90*, 3363–3372. [CrossRef]
27. de Dobbeleer, I.; Gummersbach, J.; Huebschmann, H.-J.; Mayer, A.; Silcock, P. *Analyzing PBDEs in House Dust Samples with the Thermo Scientific TSQ Quantum XLS Ultra GC-MS/MS in EI-SRM Mode*; Thermo Fisher Scientific: Dreieich, Germany, 2012; pp. 1–6.
28. Wolfe, K.; Wu, X.; Liu, R.H. Antioxidant activity of apple peels. *J. Agric. Food Chem.* **2003**, *51*, 609–614. [CrossRef]
29. Issa, N.K.; Abdul Jabar, R.; Hammo, Y.; Kamal, I. Antioxidant activity of apple peels bioactive molecules extractives. *Sci. Technol.* **2016**, *6*, 76–88.
30. Zhishen, J.; Mengcheng, T.; Jianming, W. The determination of flavonoid contents in mulberry and their scavenging effects on superoxide radicals. *Food Chem.* **1999**, *64*, 555–559. [CrossRef]
31. Burlingame, B. Wild nutrition. *J. Food Compos. Anal.* **2000**, *13*, 99–100. [CrossRef]
32. Aberoumand, A. Nutritional evaluation of edible Portulaca oleracia as plant food. *Food Anal. Methods* **2009**, *2*, 204–207. [CrossRef]
33. Devasenan, S.; Beevi, N.H.; Jayanthi, S. Green synthesis and characterization of zinc nanoparticle using Andrographis paniculata leaf extract. *Int. J. Pharm. Sci. Rev. Res.* **2016**, *39*, 243–247.
34. Otunola, G.A.; Afolayan, A.J.; Ajayi, E.O.; Odeyemi, S.W. Characterization, antibacterial and antioxidant properties of silver nanoparticles synthesized from aqueous extracts of Allium sativum, Zingiber officinale, and Capsicum frutescens. *Pharmacogn. Mag.* **2017**, *13*, S201. [CrossRef] [PubMed]
35. Bhattacharjee, S. DLS and zeta potential–what they are and what they are not? *J. Control. Release* **2016**, *235*, 337–351. [CrossRef] [PubMed]
36. Honary, S.; Zahir, F. Effect of zeta potential on the properties of nano-drug delivery systems—A review (Part 2). *Trop. J. Pharm. Res.* **2013**, *12*, 265–273.
37. Kitts, D.D.; Wijewickreme, A.N.; Hu, C. Antioxidant properties of a North American ginseng extract. *Mol. Cell. Biochem.* **2000**, *203*, 1–10. [CrossRef]
38. Abd-ElGawad, A.M.; Elshamy, A.I.; El-Amier, Y.A.; El Gendy, A.E.-N.G.; Al-Barati, S.A.; Dar, B.A.; Al-Rowaily, S.L.; Assaeed, A.M. Chemical composition variations, allelopathic, and antioxidant activities of *Symphyotrichum squamatum* (Spreng.) Nesom essential oils growing in heterogeneous habitats. *Arab. J. Chem.* **2020**, *13*, 4237–4245. [CrossRef]
39. Miguel, M.G. Antioxidant activity of medicinal and aromatic plants. A review. *Flavour Fragr. J.* **2010**, *25*, 291–312. [CrossRef]
40. Parejo, I.; Codina, C.; Petrakis, C.; Kefalas, P. Evaluation of scavenging activity assessed by Co (II)/EDTA-induced luminol chemiluminescence and DPPH·(2, 2-diphenyl-1-picrylhydrazyl) free radical assay. *J. Pharmacol. Toxicol. Methods* **2000**, *44*, 507–512. [CrossRef] [PubMed]
41. Bondock, S.; Adel, S.; Etman, H.A.; Badria, F.A. Synthesis and antitumor evaluation of some new 1,3,4-oxadiazole-based heterocycles. *Eur. J. Med. Chem.* **2012**, *48*, 192–199. [CrossRef] [PubMed]
42. El-Sheikh, T.M.; Hassan, M.I.; Moselhy, W.A.; Amer, M.S.; Shehata, A.Z. Evaluation of the biological activity of some *Cupressus sempervirens* (Cupressaceae) extracts against the mosquito vector *Culex pipiens* L. (Diptera: Culicidae). *Egypt. Acad. J. Biol. Sci. A Entomol.* **2011**, *4*, 33–48. [CrossRef]
43. Briggs, J.D. Reduction of adult house-fly emergence by the effects of *Bacillus* spp. on the development of immature forms. *J. Insect Pathol.* **1960**, *2*, 418–432.
44. Mohammed, H.A.; Ali, H.M.; Qureshi, K.A.; Alsharidah, M.; Kandil, Y.I.; Said, R.; Mohammed, S.A.; Al-Omar, M.S.; Rugaie, O.A.; Abdellatif, A.A. Comparative phytochemical profile and biological activity of four major medicinal halophytes from Qassim flora. *Plants* **2021**, *10*, 2208. [CrossRef] [PubMed]
45. Maatalah, M.B.; Bouguerra, A.; Bellila, A.; Haba, H. Chemical composition and biological activities of *Anabasis articulata* essential oil from Algeria. *J. Essent. Oil Res.* **2012**, *24*, 201–206.
46. Boukhris, S.; Nasri, R.; Bouaziz, M. Chemical composition and biological activities of *Anabasis articulata* essential oil from Tunisia. *J. Essent. Oil Bear. Plants* **2016**, *19*, 485–495.

47. Ali, M.S.; Ahmed, F.; Shahat, A.A.; Al-Yahya, M.A. Chemical constituents of *Anabasis articulata* (Forssk.) Moq. from Algeria. *Pharmacogn. J.* **2018**, *10*, 80–84.
48. Abd-ElGawad, A.M.; Ahmed, R.F.; Elshamy, A.I.; Sadek, E.G.; Assaeed, A.M.; Bonanomi, G.; El Gendy, A.E.-N.G.; El-Amier, Y.A. Achillea fragrantissima essential oil, wild grown in Saudi Arabia and Egypt: Detailed comparative chemical profiling, and evaluation of allelopathic, antioxidant, and antibacterial activities. *Chemistry* **2023**, *5*, 2347–2361. [CrossRef]
49. Gnanasangeetha, D.; Thambavani, D.S. Biogenic production of zinc oxide nanoparticles using Acalypha indica. *J. Chem. Biol. Phys. Sci. (JCBPS)* **2013**, *4*, 238.
50. Singh, J.; Dutta, T.; Kim, K.-H.; Rawat, M.; Samddar, P.; Kumar, P. 'Green' synthesis of metals and their oxide nanoparticles: Applications for environmental remediation. *J. Nanobiotechnol.* **2018**, *16*, 84. [CrossRef]
51. Ovais, M.; Khalil, A.T.; Islam, N.U.; Ahmad, I.; Ayaz, M.; Saravanan, M.; Shinwari, Z.K.; Mukherjee, S. Role of plant phytochemicals and microbial enzymes in biosynthesis of metallic nanoparticles. *Appl. Microbiol. Biotechnol.* **2018**, *102*, 6799–6814. [CrossRef] [PubMed]
52. Ghosh, S.; Patil, S.; Ahire, M.; Kitture, R.; Kale, S.; Pardesi, K.; Cameotra, S.S.; Bellare, J.; Dhavale, D.D.; Jabgunde, A. Synthesis of silver nanoparticles using Dioscorea bulbifera tuber extract and evaluation of its synergistic potential in combination with antimicrobial agents. *Int. J. Nanomed.* **2012**, *7*, 483.
53. Suhag, R.; Kumar, R.; Dhiman, A.; Sharma, A.; Prabhakar, P.K.; Gopalakrishnan, K.; Kumar, R.; Singh, A. Fruit peel bioactives, valorisation into nanoparticles and potential applications: A review. *Crit. Rev. Food Sci. Nutr.* **2022**, *63*, 6757–6776. [CrossRef]
54. Behera, A.; Awasthi, S. Anticancer, Antimicrobial and Hemolytic Assessment of Zinc Oxide Nanoparticles Synthesized from Lagerstroemia indica. *BioNanoScience* **2021**, *11*, 1030–1048. [CrossRef]
55. Salama, S.A.; Al-Faifi, Z.E.; El-Amier, Y.A. Chemical Composition of Reichardia tingitana Methanolic Extract and Its Potential Antioxidant, Antimicrobial, Cytotoxic and Larvicidal Activity. *Plants* **2022**, *11*, 2028. [CrossRef]
56. Tavakoli, R.; Mohadjerani, M.; Hosseinzadeh, R.; Tajbakhsh, M.; Naqinezhad, A. Essential-Oil and Fatty-Acid Composition, and Antioxidant Activity of Extracts of Ficaria kochii. *Chem. Biodivers.* **2012**, *9*, 2732–2741. [CrossRef]
57. Jerković, I.; Cikoš, A.-M.; Babić, S.; Čižmek, L.; Bojanić, K.; Aladić, K.; Ul'yanovskii, N.V.; Kosyakov, D.S.; Lebedev, A.T.; Čož-Rakovac, R. Bioprospecting of less-polar constituents from endemic brown macroalga Fucus virsoides J. Agardh from the Adriatic Sea and targeted antioxidant effects in vitro and in vivo (zebrafish model). *Mar. Drugs* **2021**, *19*, 235. [CrossRef]
58. Salama, S.A.; Al-Faifi, Z.E.; Masood, M.F.; El-Amier, Y.A. Investigation and Biological Assessment of *Rumex vesicarius* L. Extract: Characterization of the Chemical Components and Antioxidant, Antimicrobial, Cytotoxic, and Anti-Dengue Vector Activity. *Molecules* **2022**, *27*, 3177. [CrossRef] [PubMed]
59. Nengroo, Z.R.; Rauf, A. Fatty acid composition and antioxidant activities of five medicinal plants from Kashmir. *Ind. Crops Prod.* **2019**, *140*, 111596. [CrossRef]
60. Okwu, D.E. Citrus fruits: A rich source of phytochemicals and their roles in human health. *Int. J. Chem. Sci.* **2008**, *6*, 451–471.
61. Belyagoubi-Benhammou, N.; Belyagoubi, L.; Gismondi, A.; Di Marco, G.; Canini, A.; Atik Bekkara, F. GC/MS analysis, and antioxidant and antimicrobial activities of alkaloids extracted by polar and apolar solvents from the stems of *Anabasis articulata*. *Med. Chem. Res.* **2019**, *28*, 754–767. [CrossRef]
62. Vitaglione, P.; Napolitano, A.; Fogliano, V. Caffeic acid derivatives from Origanum vulgare protect low-density lipoprotein from oxidation in vitro. *J. Agric. Food Chem.* **2004**, *52*, 584–589.
63. El-Amier, Y.A.; Soufan, W.; Almutairi, K.F.; Zaghloul, N.S.; Abd-ElGawad, A.M. Proximate Composition, Bioactive Compounds, and Antioxidant Potential of Wild Halophytes Grown in Coastal Salt Marsh Habitats. *Molecules* **2021**, *27*, 28. [CrossRef]
64. Zaki, A.A.; Al-Karmalawy, A.A.; Khodir, A.E.; El-Amier, Y.A.; Ashour, A. Isolation of cytotoxic active compounds from Reichardia tingitana with investigation of apoptosis mechanistic induction: In silico, in vitro, and SAR studies. *S. Afr. J. Bot.* **2022**, *144*, 115–123. [CrossRef]
65. Havelek, R.; Muthna, D.; Tomsik, P.; Kralovec, K.; Seifrtova, M.; Cahlikova, L.; Hostalkova, A.; Safratova, M.; Perwein, M.; Cermakova, E. Anticancer potential of Amaryllidaceae alkaloids evaluated by screening with a panel of human cells, real-time cellular analysis and Ehrlich tumor-bearing mice. *Chem.-Biol. Interact.* **2017**, *275*, 121–132. [CrossRef] [PubMed]
66. Mitra, S.; Subia, B.; Patra, P.; Chandra, S.; Debnath, N.; Das, S.; Banerjee, R.; Kundu, S.C.; Pramanik, P.; Goswami, A. Porous ZnO nanorod for targeted delivery of doxorubicin: In vitro and in vivo response for therapeutic applications. *J. Mater. Chem.* **2012**, *22*, 24145–24154. [CrossRef]
67. Cai, X.; Luo, Y.; Zhang, W.; Du, D.; Lin, Y. pH-Sensitive ZnO quantum dots–doxorubicin nanoparticles for lung cancer targeted drug delivery. *ACS Appl. Mater. Interfaces* **2016**, *8*, 22442–22450. [CrossRef]
68. Raha, S.; Ahmaruzzaman, M. ZnO nanostructured materials and their potential applications: Progress, challenges and perspectives. *Nanoscale Adv.* **2022**, *4*, 1868–1925. [CrossRef] [PubMed]
69. Zhang, Y.; R Nayak, T.; Hong, H.; Cai, W. Biomedical applications of zinc oxide nanomaterials. *Curr. Mol. Med.* **2013**, *13*, 1633–1645. [CrossRef] [PubMed]
70. Martínez-Carmona, M.; Gun'Ko, Y.; Vallet-Regí, M. ZnO nanostructures for drug delivery and theranostic applications. *Nanomaterials* **2018**, *8*, 268. [CrossRef] [PubMed]
71. Gao, Y.; Arokia Vijaya Anand, M.; Ramachandran, V.; Karthikkumar, V.; Shalini, V.; Vijayalakshmi, S.; Ernest, D. Biofabrication of zinc oxide nanoparticles from *Aspergillus niger*, their antioxidant, antimicrobial and anticancer activity. *J. Clust. Sci.* **2019**, *30*, 937–946. [CrossRef]

72. Gray, E.; Bradley, T. Malarial infection in Aedes aegypti: Effects on feeding, fecundity and metabolic rate. *Parasitology* **2006**, *132*, 169–176. [CrossRef] [PubMed]
73. Franklinos, L.H.; Jones, K.E.; Redding, D.W.; Abubakar, I. The effect of global change on mosquito-borne disease. *Lancet Infect. Dis.* **2019**, *19*, e302–e312. [CrossRef]
74. Manimaran, K.; Balasubramani, G.; Ragavendran, C.; Natarajan, D.; Murugesan, S. Biological applications of synthesized zno nanoparticles using Pleurotus djamor against mosquito larvicidal, histopathology, antibacterial, antioxidant and anticancer effect. *J. Clust. Sci.* **2021**, *32*, 1635–1647. [CrossRef]
75. Patil, C.D.; Borase, H.P.; Patil, S.V.; Salunkhe, R.B.; Salunke, B.K. Larvicidal activity of silver nanoparticles synthesized using Pergularia daemia plant latex against Aedes aegypti and Anopheles stephensi and nontarget fish Poecillia reticulata. *Parasitol. Res.* **2012**, *111*, 555–562. [CrossRef] [PubMed]
76. Santhosh, S.; Yuvarajan, R.; Natarajan, D. Annona muricata leaf extract-mediated silver nanoparticles synthesis and its larvicidal potential against dengue, malaria and filariasis vector. *Parasitol. Res.* **2015**, *114*, 3087–3096. [CrossRef]
77. Murugan, K.; Benelli, G.; Panneerselvam, C.; Subramaniam, J.; Jeyalalitha, T.; Dinesh, D.; Nicoletti, M.; Hwang, J.-S.; Suresh, U.; Madhiyazhagan, P. Cymbopogon citratus-synthesized gold nanoparticles boost the predation efficiency of copepod Mesocyclops aspericornis against malaria and dengue mosquitoes. *Exp. Parasitol.* **2015**, *153*, 129–138. [CrossRef]
78. Murugan, K.; Jaganathan, A.; Rajaganesh, R.; Suresh, U.; Madhavan, J.; Senthil-Nathan, S.; Rajasekar, A.; Higuchi, A.; Kumar, S.S.; Alarfaj, A.A. Poly (styrene sulfonate)/poly (allylamine hydrochloride) encapsulation of $TiO_2$ nanoparticles boosts their toxic and repellent activity against zika virus mosquito vectors. *J. Clust. Sci.* **2018**, *29*, 27–39. [CrossRef]


**Disclaimer/Publisher's Note:** The statements, opinions and data contained in all publications are solely those of the individual author(s) and contributor(s) and not of MDPI and/or the editor(s). MDPI and/or the editor(s) disclaim responsibility for any injury to people or property resulting from any ideas, methods, instructions or products referred to in the content.